

Assessment of the Crustal Thickness within Southern Bida Basin and Surrounding Basement Rocks, North Central Nigeria, using Gravity Data

*Jimoh, N. L. and Udensi, E. E.



Department of Physics, School of Physical Sciences, Federal University of Technology, Minna, Niger State, Nigeria.

*Corresponding author's email: lawalnussy@gmail.com Phone: +2348032853554

ABSTRACT

The crustal thickness within the Southern Bida Basin has been determined using Bouguer Gravity Data. This study focuses on a region situated in the southern part of the Bida Basin, a significant inland sedimentary basin in North Central Nigeria. Two distinct methods were employed to estimate crustal thickness from Bouguer anomaly values: (i) an empirical relationship between crustal thickness and Bouguer anomaly, and (ii) spectral analysis of the radial wave number. The average crustal thickness was derived by averaging results obtained from both methods. Additionally, a linear equation ($HC = 34.39 - 0.17BG$) was formulated for the study area, enabling straightforward determination of crustal thickness from any given Bouguer anomaly value. The estimated crustal thickness in the study area ranges from 32 km to 40 km, aligning closely with the overall crustal thickness of Nigeria as reported by Daniyan et al. (2002). The tectonic stability of the study area, situated on the stable African plate, further underscores its significance within the broader geological context of Nigeria.

Keywords:

Bouguer anomaly,
Crustal,
Spectral,
Empirical

INTRODUCTION

The determination of crustal thickness is a fundamental geophysical challenge in the North Central part of Nigeria. Understanding the stability of Earth's crust is essential in tackling this issue. Earth, the densest planet in the solar system, is the third planet from the sun and the largest among the four terrestrial planets. It is also the only planet known to support life (www.coatal.gov). The Earth's structure, as revealed by seismology, consists of three main zones: the core, the mantle, and the crust (Figure 1a). The boundary between the Earth's crust and mantle is known as the *Mohorovičić* discontinuity, or Moho. In geology, a "discontinuity" refers to surfaces where seismic waves change velocity. The Moho is typically found approximately 8 km below ocean basins and about 32 km below continents. Andrija *Mohorovičić*, a Croatian seismologist, discovered the Moho in 1909. He observed that the speed of seismic waves correlates with the density of the materials they

travel through, indicating compositional changes within Earth's outer layers (www.geology.com). The acceleration is likely caused by the presence of higher-density materials at depth. The red line in Figure 1a marks the location of the Moho, which signifies the boundary between Earth's crust and mantle. The outermost layer of Earth is known as the crust, comprising just one percent of the planet's total mass. It is the solid, rocky layer upon which life exists, divided into two distinct types: oceanic crust and continental crust. Oceanic crust constitutes 71 percent of Earth's crust, while the remaining percentage is covered by continental crust. Igneous rocks primarily from the continental crust, whereas sedimentary and basaltic rocks characterize the oceanic crust. The crust is in constant motion and serves as the exclusive layer where tectonic plate activity occurs or originates (www.hubpages.com).

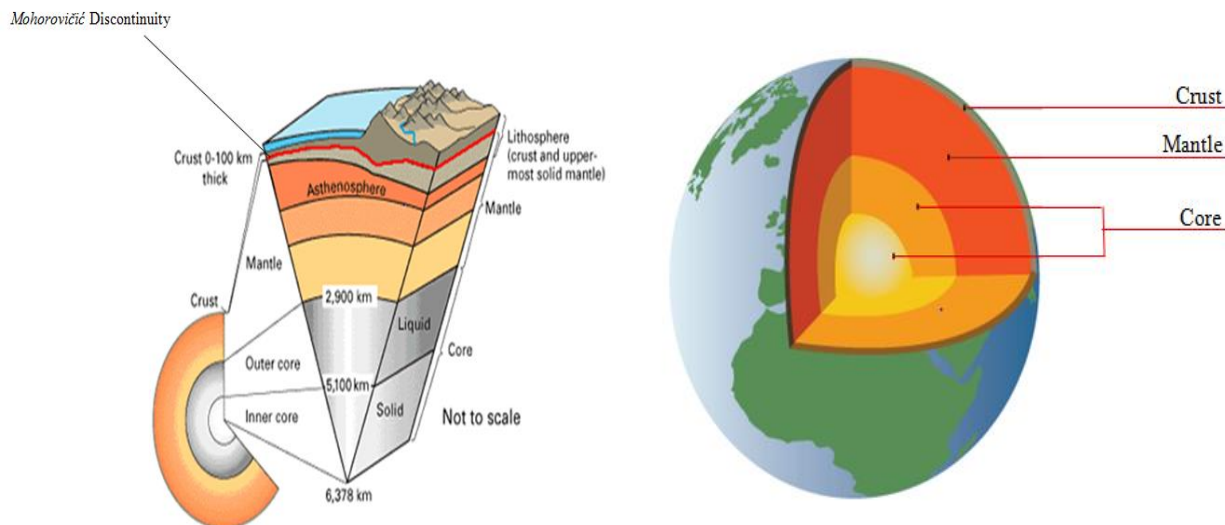


Figure 1: (a) Cross sectional structure of the earth and (b) The internal structure of Earth by USGS - Mohorovičić Discontinuity

Consequently, its thickness varies significantly from one location to another. Understanding the crustal thickness in a region provides valuable insights into the thickness of the lithosphere, the Earth's rigid outer layer. Variations in crustal thickness also indicate the level of tectonic stability or instability in an area. This research aims to determine the crustal thickness within the study area to assess its tectonic stability. The Moho is recognized as the boundary between the Earth's crust and mantle (Lewis, 1983). While accurate imaging of this interface typically requires costly deep seismic profiling, economic considerations often favor the use of gravity methods for estimating crustal thickness, provided that available geological and geophysical data offer a reasonable approximation of reality. The gravity method is a non-destructive geophysical technique that measures variations in the Earth's gravitational field at specific locations. Gravity measurements reveal fluctuations in the gravitational field due to lateral differences in subsurface density (rock) or the presence of natural voids and man-made structures. This method is effective for mapping large-scale geological features across extensive areas and detecting smaller, shallow features beneath the Earth's surface (Astim, 2010). In the context of this study, gravity datasets were employed to estimate crustal thickness within the study area (Southern Bida Basin) using empirical and power spectral techniques.

Location and Geology of the Study Area

Geographically, the Bida Basin, also known as the Middle Niger Basin or Nupe Basin, is located in the north-central part of Nigeria and is divided into two sections: the Northern Bida Basin and the Southern Bida Basin. This division likely stems from rapid changes in

sedimentary facies across the basin (Olusola *et al.*, 2011).

The study area is located in the southern part of the Bida Basin, a significant inland sedimentary basin in Nigeria as depicted in Figure 2. It is bounded by latitudes $7^{\circ}00'N$ to $8^{\circ}30'N$ and longitudes $4^{\circ}00'E$ to $7^{\circ}00'E$, covering an approximate area of $54,450 \text{ km}^2$. The Bida Basin itself is an elongated depression trending northwest-southeast, characterized by a sedimentary fill thickness of approximately three kilometers (3 km). This basin stretches from Kontagora in the north to Lokoja in the south. Positioned nearly perpendicular to the primary axis of the Benue Trough, it is separated from the Sokoto Basin's basal continental bed by a narrow exposure of crystalline basement rocks to the west, and it is adjacent to the Anambra Basin on the east. Geologically, Figure 2 depicts the study area, which is characterized by Pre-Cambrian to lower Paleozoic basement rocks such as gneisses, migmatites, and metasedimentary schists overlain by a sequence of sandstones, shales, siltstones, and ironstones (Obaje, 2009; Obaje *et al.*, 2011). The Pre-Cambrian basement rocks underwent significant deformation during the late Pan-African phase, forming megashears that were later reactivated during the late Campanian-Maastrichtian period (Braide, 1990). Gneisses and metasedimentary schists predominantly occur as flat-lying outcrops (Shekwolo, 1992). The sandstones consist of cemented fine to coarse-grained particles, often interbedded with thin layers of carbonaceous shales and clays. The stratigraphy in the study area includes the basal Lokoja Formation, followed by the Patti Formation, and topped by the Agbaja Formation.

MATERIALS AND METHODS

The commonly utilized processed gravity data in geophysics are referred to as *Bouguer* gravity anomaly data. The *Bouguer* gravity data for the study area were collected through a comprehensive gravity survey conducted by a team, primarily aimed at determining

Nigeria's crustal thickness. These data underwent corrections to standardize gravity measurements to a datum equipotential surface. Gravity readings are typically affected by various factors including latitude, elevation, local topography, earth tides, and variations in subsurface density.

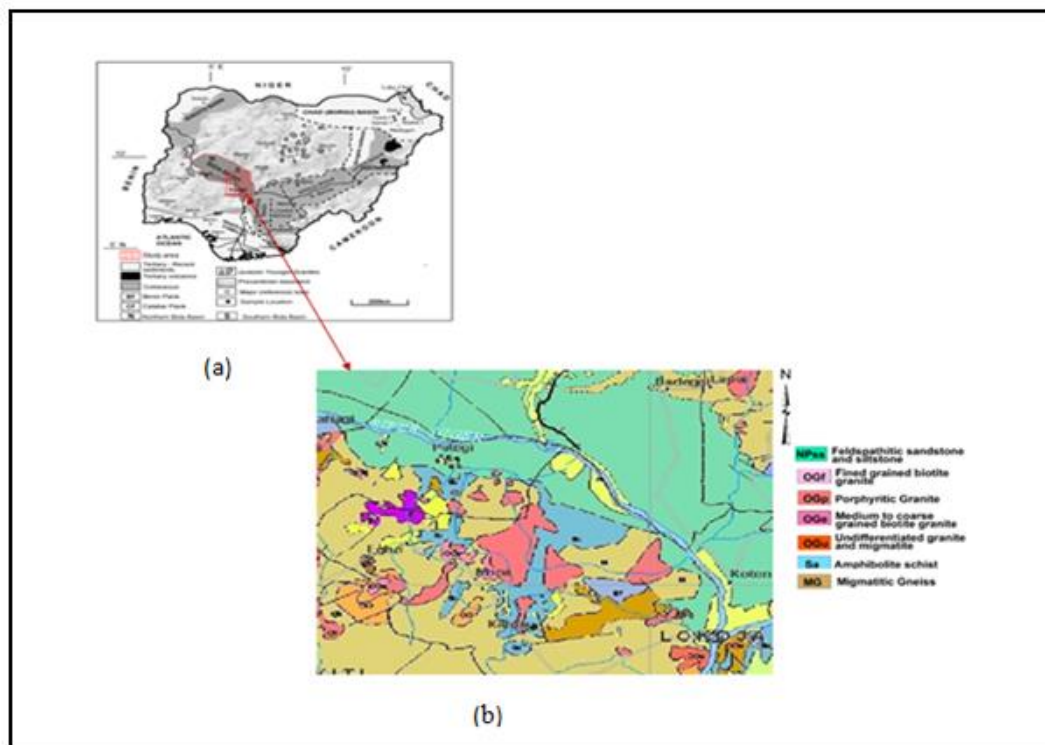


Figure 2: Location of the Study Area (in red rectangle) on a Sketched Geological Map of Nigeria (Modified from Obaje, 2009a); (b) Digitized Geological Map of the Study Area extracted from the Geological Map of Nigeria prepared by NGSA (2009).

Observed Gravity (g_{obs})

The gravity readings observed at each gravity station have been corrected for instrument drift and Earth tides.

Latitude correction (g_n)

Latitude corrections typically involve subtracting the normal gravity, calculated using the International Gravity Formula, from the observed gravity readings. This correction accounts for the Earth's oblate shape and rotation. Normal gravity represents the theoretical gravity value that would be observed if Earth were a perfect, uniformly rotating ellipsoid without any geological or topographic irregularities (Bauer *et al.*, 1999).

$$g_n = 978031.85 (1.0 + 0.005278895 \sin^2(\text{lat}) + 0.000023462 \sin^4(\text{lat})) \text{ (in mGal)} \quad (1)$$

The equation (1) provided calculates the normal gravity (g_n) as a function of latitude (lat). Here's a breakdown of the formula. In this equation:

g_n is the normal gravity in milliGals (mGal).

lat is the latitude in degrees.

The formula incorporates a latitude-dependent correction factor to the standard gravitational acceleration (978031.85 mGal), accounting for the Earth's oblate shape and rotational effects. The terms $\sin^2(\text{lat})$ and $\sin^4(\text{lat})$ adjust for the variations in gravity due to the Earth's equatorial bulge and are used to compute the normal gravity value at specific latitude.

Free-Air Correction (g_{fa})

The residual gravity anomaly, known as the Free-Air gravity anomaly (g_{fa}), is computed by subtracting the normal gravity (g_n), calculated from the International Gravity Formula, from the observed gravity (g_{obs}). Additionally, a correction term is added to account for the effect of elevation (h) above the sea-level reference surface (Bauer *et al.*, 1999). The formula for the Free-Air gravity anomaly is:

$$g_{fa} = g_{obs} - g_n + 0.3086h \text{ (in mGal)} \quad (2)$$

This correction term, $0.3086h$, adjusts for gravity variations due to differences in elevation at the observation locations. The Free-Air gravity anomaly (g_a) is calculated by subtracting the normal gravity (g_n), derived from the International Gravity Formula, from the observed gravity (g_{obs}). An additional term, $0.3086h$, adjusts for the effect of elevation (h) above the sea-level reference surface where the gravity station is located. This elevation correction accounts for variations in gravity due to differences in height relative to the datum, typically sea level.

Bouguer Correction (g_b)

The Bouguer gravity anomaly (g_b) is a refined measure that includes corrections for both elevation and the density of subsurface rocks. It is derived by subtracting the normal gravity (g_n) from the observed gravity (g_{obs}), and then adjusting for elevation effects with $0.3086h$. Additionally, a Bouguer correction factor, which considers the average density (ρ) of rocks beneath the survey area, is subtracted. This correction accounts for the gravitational impact of the mass beneath observation points, whether there is an excess mass (at higher elevations) or a deficiency (at lower elevations) relative to the elevation datum (typically sea level or the geoid) (Bauer *et al.*, 1999). The formula for the Bouguer gravity anomaly is:

$$g_b = g_{obs} - g_n + 0.3086h - 0.04193\rho h \text{ (mGal)} \quad (3)$$

Here, ρ represents the average density of the rocks underlying the survey area, and h is the elevation of the gravity station above the reference surface (sea level or geoid). This formula provides a more accurate measurement of gravity anomalies by accounting for the gravitational effects of both elevation differences and subsurface rock density variations.

Terrain Corrections (T_c)

The Terrain corrected Bouguer gravity anomaly (g_t) adjusts for gravitational variations caused by the uneven topography near each observation point. It enhances the Bouguer gravity anomaly (g_b) by incorporating a correction factor (T_c) that compensates for the effects of local terrain. This correction is crucial because the simple assumptions underlying the Bouguer slab correction method can lead to inaccuracies, whether the terrain is mountainous or a valley (Bauer *et al.*, 1999). The formula for the Terrain corrected Bouguer gravity anomaly is:

$$g_t = g_{obs} - g_n + 0.3086h - 0.04193\rho h + T_c \text{ (in mGal)} \quad (4)$$

Here, g_{obs} is the observed gravity, g_n is the normal gravity, h is the elevation of the gravity station above the reference surface, ρ is the average density of the rocks underlying the survey area, and T_c is the computed terrain correction.

Equation (4) provides a more precise measurement of gravity anomalies by accounting for both elevation

differences and the local variations in topography near each measurement point. Assuming that corrections for variations in gravitational acceleration due to latitude and topography have been accurately applied, any residual variations in gravitational acceleration can be attributed to geological structures. The difference between the observed gravity at a location and its theoretical value based on latitude is referred to as the gravity anomaly (Mishra, 2000). There are two primary types of gravity anomalies: Free Air and Bouguer anomalies (Mishra, 2000). The Free Air Gravity Anomaly (Δg_f) represents the observed gravity field after corrections have been made for latitude (theoretical gravity), tidal effects, and topography (Bauer *et al.*, 1999). It is expressed as:

$$\Delta g_f = \text{observed gravity} - \text{tidal correction} - \text{theoretical gravity} + \text{topographic correction} + \text{free air correction} \quad (5)$$

Equation (5) accounts for the various corrections needed to refine the observed gravity measurements, ensuring that the resulting Free Air Gravity Anomaly (Δg_f) provides a clearer depiction of gravitational anomalies influenced primarily by geological structures in the surveyed area. The corrected gravity field, known as the Bouguer Gravity Anomaly (Δg), is obtained by subtracting the attraction due to the material between the observation plane and the Bouguer correction (g_b) from the Free Air Gravity Anomaly (Δg_f) (Bauer *et al.*, 1999). Mathematically, it is expressed as:

$$\Delta g = \Delta g_f - g_b \quad (6)$$

Here, Δg_f is the Free Air Gravity Anomaly, and g_b is the Bouguer Gravity Anomaly.

This calculation yields the Bouguer Gravity Anomaly (Δg), which represents the residual gravity anomaly after correcting for the effects of latitude, topography, and subsurface rock density variations. The Bouguer Gravity Anomaly is particularly useful in geophysical investigations as it provides a clearer indication of subsurface geological structures and compositions. The Bouguer gravity anomaly values demonstrate a consistent relationship between crustal structure, crustal density, and surface elevation (Tealeb and Riad, 1986). At a regional scale, these anomalies are sufficiently distinct to indicate variations in mass discontinuities within the Earth's crust and mantle (Tealeb and Riad, 1986). Subsequently, the corrected data, consisting of longitude (x), latitude (y), and their corresponding Bouguer gravity anomaly values (z), which were stored in a computer storage device, were imported into the Geosoft® Oasis Montaj™ software package via an Excel spreadsheet. Within the Geosoft® Oasis Montaj™ environment, the Bouguer gravity anomaly values (z) were gridded using the minimum curvature method. This process was conducted to visually present the precise sizes and shapes of the anomalies, facilitating further interpretation and analysis.

Determination of Crustal Thickness using Empirical Relations

Three empirical relations that show a linear relationship between crustal thickness (H) in kilometers and Bouguer gravity anomaly (BG) in milligals (mGal) for the whole Earth, as developed by Demenistskaya (1958), Woolard (1959), and Woolard and Strange (1962) are represented respectively as:

$$H_D = 35(1 - \text{Tanh}(0.037BG)) \quad (7)$$

$$H_W = 32.0 - 0.08BG \quad (8)$$

$$H_{WS} = 40.50 - 32.50 \text{Tanh}\left(\frac{BG+75}{275}\right) \quad (9)$$

In equations (7), (8), and (9),

H is the crustal thickness in kilometers (km),

BG is the Bouguer gravity anomaly in milligals (mGal).

These empirical relations provide a straightforward way to estimate crustal thickness based on Bouguer gravity anomaly measurements, offering useful tools in geophysical studies and exploration. From equations (7), (8), and (9), let

$$(0.037BG) = X \quad (10)$$

$$0.08BG = Y \quad (11)$$

$$\frac{BG+75}{275} = Z \quad (12)$$

Recall that the hyperbolic function is,

$$\text{Tanh } X = \frac{\text{Sinh } X}{\text{Cosh } X} \quad (13)$$

$$\text{Where } \text{Sinh } X = \frac{e^x - e^{-x}}{2} \quad (14)$$

$$\text{Cosh } X = \frac{e^x + e^{-x}}{2} \quad (15)$$

$$\text{Therefore, } \text{Tanh } X = \frac{e^x - e^{-x}}{e^x + e^{-x}} \quad (16)$$

In other words, equation (7), (8) and (9) becomes

$$H_D = 35\left(1 - \left(\frac{e^x - e^{-x}}{e^x + e^{-x}}\right)(0.037BG)\right) \quad (17)$$

$$H_W = 32.0 - (0.08BG) \quad (18)$$

$$H_{WS} = 40.50 - 32.50\left(\frac{e^x - e^{-x}}{e^x + e^{-x}}\left(\frac{BG+75}{275}\right)\right) \quad (19)$$

In this study, the equations developed by Demenistskaya (1958), Woolard (1959), and Woolard and Strange (1962) were utilized to determine the crustal thickness of the study area. These empirical relationships provide a method to estimate crustal thickness based on Bouguer gravity anomaly data. To determine the crustal thickness at specific locations within the study area, average values derived from these empirical equations were calculated. These averages were then used to create contour maps using the "SURFER 10" graphical package. This approach allows visualization of the spatial distribution of crustal thickness across the study area. It's noteworthy that similar empirical relations have been employed by Daniyan et al. (2002) and Udensi (2000) in estimating the crustal thickness for the entire country of Nigeria. This indicates the reliability and applicability of these equations in geophysical studies across different regions and scales.

Determination of Crustal Thickness using Power Spectrum Method

This is a statistical technique used to analyze large gravity datasets by transforming them from the space domain to the frequency domain using 2-D Fast Fourier Transform (FFT). This method helps in quantitatively assessing the depth of geological sources and detecting discontinuities in the subsurface. Spector and Grant (1970) pioneered the use of power spectrum analysis to determine the average depths of magnetic layers. They plotted the logarithm of the power of magnetic anomalies against wave number to analyze the frequency content of the data. Syberg (1972) and later Poudjom Djomani *et al.* (1995) adapted and improved this method to estimate crustal thickness using gravity data. In this study, similar methods were employed to analyze Bouguer gravity data in the wave-number domain. The Moho depth (d), which represents the boundary between the Earth's crust and mantle, is calculated using specific equations derived from the analysis of the power spectrum Poudjom Djomani *et al.* (1995).

$$d = \frac{mM}{2\pi} K \quad (20)$$

Where, 'd' is the Moho depth, typically expressed in kilometers (km), 'K' is the wave number, which represents the spatial frequency of the anomalies detected in the gravity data, 'm' is the slope of the average power spectrum. It characterizes the rate at which the power of the anomalies decreases with increasing wave number and 'N' is the number of gravity data points used in the analysis.

This equation shows how the Moho depth can be derived from the analysis of the power spectrum of Bouguer gravity anomalies. The process involves plotting the logarithm of the power spectrum against the wave number, which helps in visualizing the frequency content of the gravity data. The analysis and plotting of the logarithm of the power spectrum against wave number were conducted using the "OASIS MONTAJ" software. This software package is commonly used for geophysical data processing and interpretation, including gravity data analysis.

RESULTS AND DISCUSSION

Qualitative Interpretation of the Bouguer Gravity Anomaly Map of the Study Area

The Bouguer gravity anomaly map (Figure 3) of the study area reveals a pattern characterized by both positive and negative anomalies with distinct closures. These closures suggest structural alignments likely influenced by tectonic activities in the region. Understanding these anomalies is crucial for interpreting the geological features and predicting future geological movements.

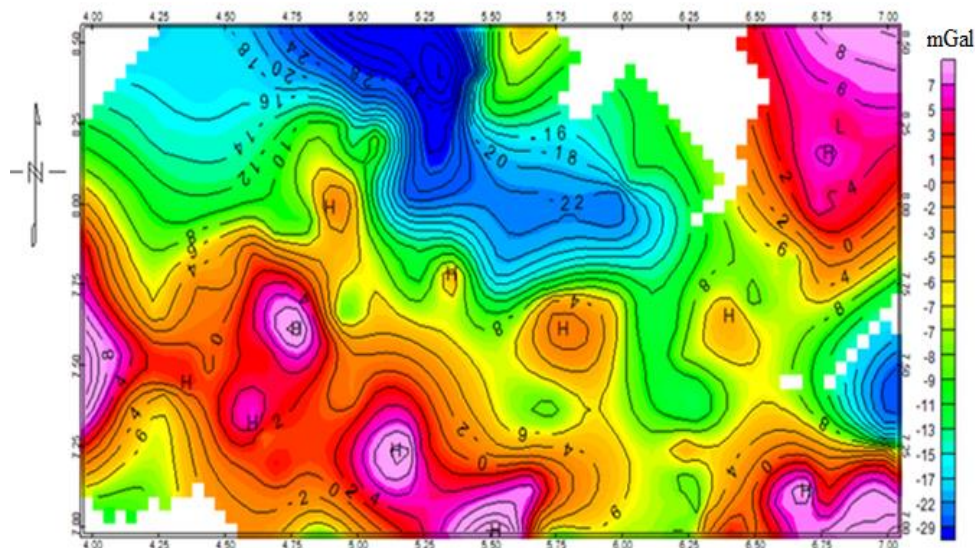


Figure 3: Bouguer Gravity Anomaly Map of the Study Area. Contour Interval is 2 mGal; Colour Bar at the Right indicates Interval Values and the Anomaly Intensity

Areas with negative Bouguer anomalies typically indicate lower-density bodies within the subsurface or extensive sedimentary deposits (sedimentary cover). These anomalies can highlight areas where sedimentary layers are relatively thick or where less dense materials are present. Positive Bouguer anomalies often indicate regions with higher-density bodies or the presence of denser materials beneath shallow sedimentary covers. These anomalies might signify areas where intrusive igneous rocks or basic intrusions exist beneath the surface. In some directions on the map, such as towards the North, South, and East, anomalies are not observed, possibly due to the presence of rivers or other geographical features that affect the gravity measurements. Figure 3 shows closures of high Bouguer anomalies denoted by 'H', which are more prevalent compared to low anomalies denoted by 'L'. These closures could signify intrusive geological formations that have penetrated through the sedimentary cover. Interpreting the Bouguer gravity anomaly map (Figure 3) is crucial for identifying and understanding the geological parameters responsible for these anomalies. It aids in deducing the geological history of the area and provides insights for predicting future geological movements and activities.

In other words, Figure 3 shows variations in Bouguer gravity anomalies across the study area. Positive anomalies indicate regions of higher density or intrusions, while negative anomalies suggest areas with lower density or sedimentary cover. Closures and patterns observed on this map are indicative of structural alignments influenced by tectonic activities. Overall, the Bouguer gravity anomaly map serves as a valuable tool for geoscientists to unravel the subsurface

geological structures, assess potential mineral resources, and make informed decisions in geological exploration and resource management.

Empirical Relation Result

Table 1 displays the results obtained from applying the empirical relation formulas that establish a linear relationship between crustal thickness (H) and Bouguer anomaly value (BG). The equations used are mentioned above. These equations were applied to the Bouguer anomaly values obtained from the study area. The resulting crustal thickness values were contoured using "SURFER 10", a software package used for creating maps and visualizing geospatial data.

Figures 4, 5, and 6 depict the crustal thickness maps generated from the empirical relation formulas by Demenitskaya (1958) (H_D), Woolard (1959) (H_W), and Woolard and Strange (1962) (H_{WS}) respectively. Each of the maps is essential for geological interpretation, resource assessment, and understanding the subsurface characteristics of the study area based on gravity data analysis and empirical relations. These maps provide a visual representation of how crustal thickness varies spatially across the study area based on the Bouguer anomaly data and the chosen empirical relations. Furthermore, the contour maps (Figures 4, 5, and 6) produced from Table 1 serve several purposes: They illustrate the spatial distribution of crustal thickness based on different empirical models. They help identify areas with thicker or thinner crust within the study area. They provide insights into the geological structure and tectonic activity inferred from crustal thickness variations. Differences in crustal thickness values at the same location across these maps (figures 4, 5 and

reflect variations due to the different empirical formulas used.

At each geographical point within the study area (from Table 1), there are three different crustal thickness values corresponding to each empirical formula. To derive a single representative crustal thickness value for each location, the arithmetic mean (average) of the three

values obtained from H_D , H_W , and H_{WS} were calculated. In other words, the process of averaging the crustal thickness values derived from the three empirical relation formulas (H_D , H_W , and H_{WS}) was used to produce a single representative value at each geographical location within the study area.

Table 1: Results Obtained by using the Formulae Developed by Demenitskaya (1958) (H_D), Woolard (1959) (H_W) and Woolard and Strange (1962) (H_{WS})

Longitude (Degree)	Latitude (Degree)	H_D (Km)	H_W (Km)	H_{WS} (Km)	Average (Km)
5.71	7.01	36.811	32.112	32.0037	33.64236564
6.26	7.03	46.59	32.744	32.8799	37.40451074
4.85	7.03	41.527	32.408	32.4125	35.4492429
6.99	7.03	22.272	31.176	30.7304	28.05941194
6.47	7.03	37.456	32.152	32.0588	33.88908334
6.32	7.03	37.843	32.176	32.0919	34.0368639
6.35	7.03	40.522	32.344	32.3239	35.06329269
6.38	7.03	34.741	31.984	31.8278	32.85094102
6.4	7.03	35.129	32.008	31.8608	32.99941914
6.43	7.03	34.612	31.976	31.8168	32.80145288
6.3	7.04	41.151	32.384	32.3793	35.30490933
6.5	7.04	34.871	31.992	31.8388	32.90043223
6.98	7.04	22.724	31.208	30.7734	28.23504974
6.27	7.05	42.645	32.48	32.5124	35.87906603
6.53	7.05	32.544	31.848	31.6415	32.0110231
6.96	7.05	22.951	31.224	30.795	28.32346543
6.55	7.05	30.111	31.696	31.4341	31.08040904
6.2794	7.0561	46.474	32.736	32.8687	37.3596411
6.25	7.06	43.259	32.52	32.5679	36.11560053

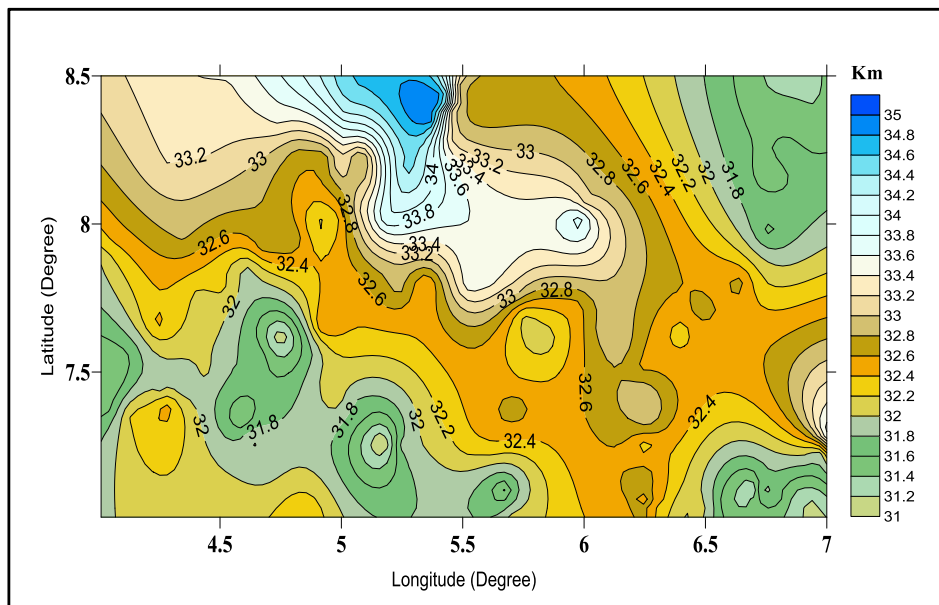


Figure 4: Demenitskaya (1958) (H_D) Contour Map of Crustal Thickness of the Study Area. [Contour Interval is 2 km. Colour Bar at the Right Indicate Values of the Crustal Thickness in the Area]

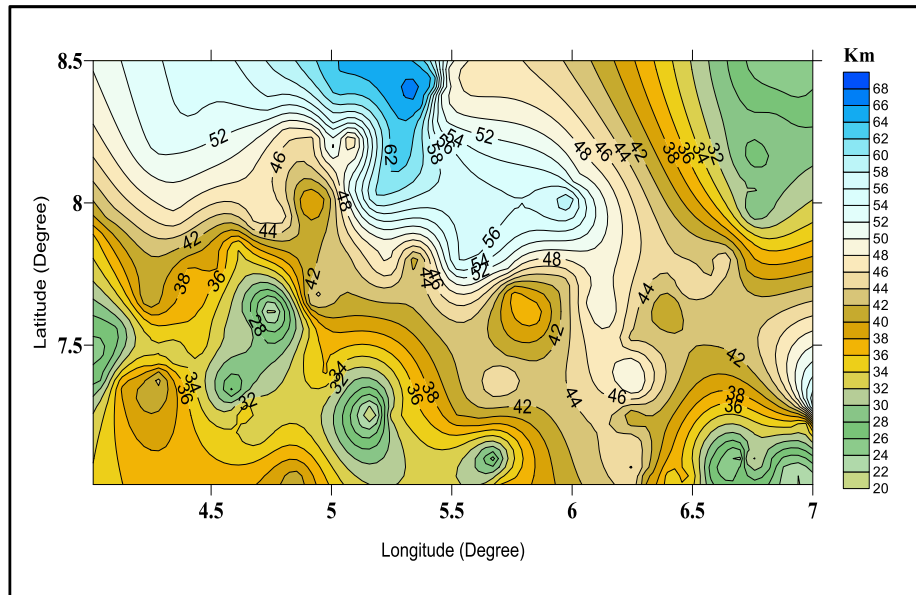


Figure 5: Woolard (1959) (H_w) Contour Map of Crustal Thickness of the Study Area. Contour Interval is 0.2 km. Colour Bar at the Right Indicate Values of the Crustal Thickness in the Area

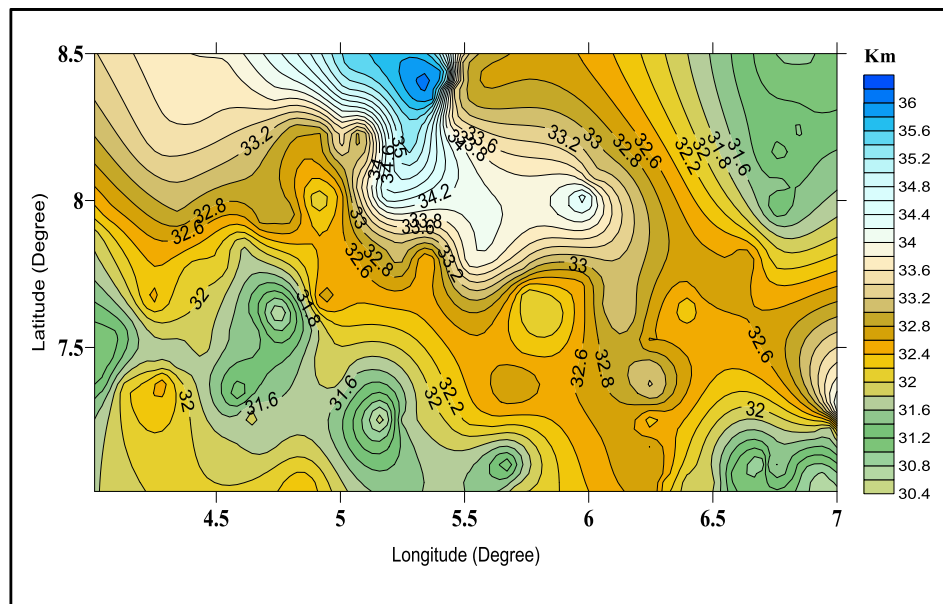


Figure 6: Woolard and Strange (1962) (H_{ws}) Contour Map of Crustal Thickness of the Study Area. Contour Interval is 0.2 km. Colour Bar at the Right Indicate Values of the Crustal Thickness in the Area]

Figure 7, displays the average crustal thickness values across the study area. The map (Figure 7) provides a consolidated view of crustal thickness trends, where each point represents a calculated average from the three empirical methods. The range of crustal thickness values (31 km to 43 km) observed in map reflects the

variability across the study area, considering the influence of geological structures and tectonic activities. Moderately high crustal values are likely attributed to high-density bodies or low sediment accumulation. Conversely, low crustal values may be due to low-density bodies or high sediment accumulation.

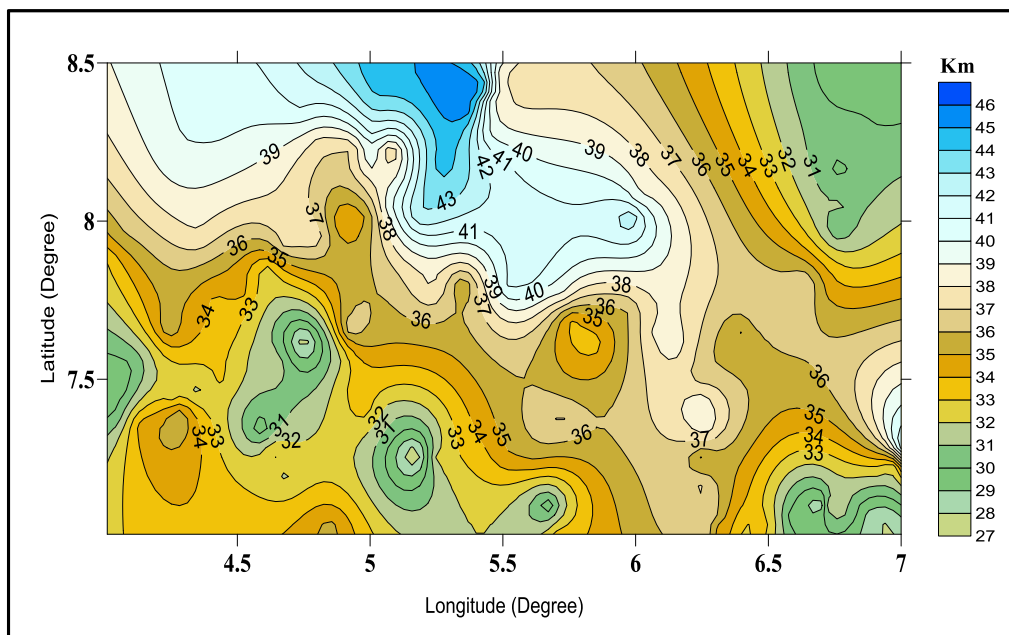


Figure 7: Average Crustal Thickness Map of the Study Area from Empirical Method. [Contour Interval is 1 km. Colour Bar at the Right Indicate Values of the Crustal Thickness in the Area]

Comparatively, Bouguer Gravity Anomaly Map (Figures 3) and Average Crustal Thickness Map (Figure 7) of the study area trend similarly in terms of spatial patterns and directions. Areas with lower Bouguer anomaly values (Figures 3), indicating reduced density or sedimentary cover, typically correspond to higher average crustal thickness values (Figure 7). Conversely, in areas where Bouguer anomaly values are high (indicating denser material or intrusions), the average crustal thickness values shown in Figure 7 tend to be lower. This comparative analysis is instrumental in geological interpretation, resource exploration, and enhances understanding of subsurface dynamics.

Figures 4, 5, and 6 provide detailed crustal thickness variations using empirical formulas, while Figures 3 and 7 provide broader insights into the geological and tectonic characteristics of the study area based on Bouguer gravity anomalies and average crustal thickness values. Together, these maps facilitate a comprehensive understanding of subsurface geological structure, aid in identifying potential resource-rich areas, and contribute to predicting geological movements within the study region.

Power Spectrum Analysis

Figure 8 depicts the logarithm of the power spectrum plotted against frequency, providing a radial wave analysis to estimate average crustal thickness. Within the plot, three straight-line segments labeled as $\text{slope}_{(1)}$, $\text{slope}_{(2)}$, and $\text{slope}_{(3)}$ correspond to different depths of anomalous sources: H_1 near the surface, H_2 at the Conrad discontinuity (the boundary between upper and lower crust), and H_3 at the Moho (the boundary between crust and mantle). These segments' slopes estimate the thicknesses of these respective geological layers. H_1 signifies the shallowest depth, H_2 represents the intermediate depth to the Conrad, and H_3 denotes the deepest point, the crustal thickness to the Moho. The logarithm of the power spectrum shows a decrease in amplitude with increasing frequency. Given the study's focus on determining H_3 , the equation below was utilized to estimate the crustal thickness of the study area:

$$H_3 = \frac{-\text{slope}_{(3)}}{2\pi} \quad (21)$$

Equation (21) leverages the slope of the segment labeled as $\text{slope}_{(3)}$ to derive the crustal thickness (H_3), which represents the deepest geological layer of interest—the boundary between the crust and mantle (Moho).

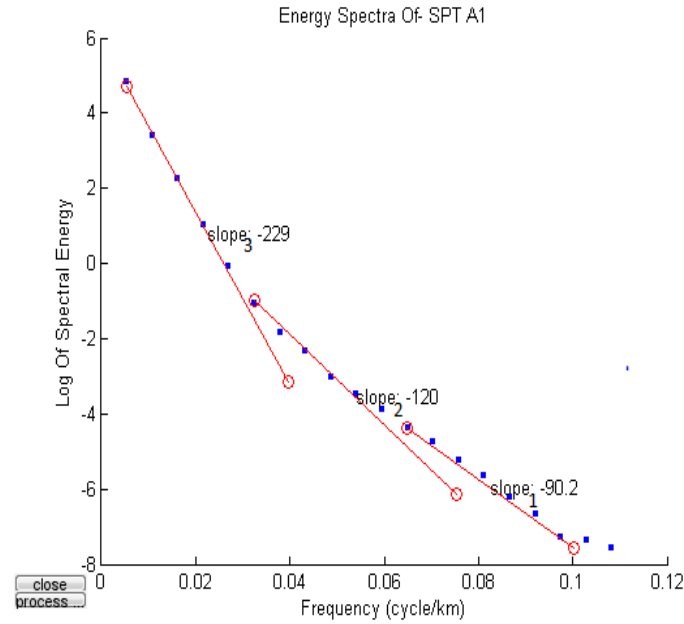


Figure 8: Plot of the Log of Spectral Energy against Frequency

Figure (9) displays the distribution of H_3 values (crustal thickness) across the study area. The map indicates that the maximum thickness of 38 km is located in the southern part, whereas the minimum thickness of 32 km is observed towards the northern edge of the study area. This spatial variation provides insights into the geological structure and crustal composition across the region, highlighting areas of significant crustal thickness variation.

Figure 10 visually represents the spatial distribution of crustal thickness across the entire study area. It

illustrates variations in crustal thickness, providing a comprehensive overview of the geological structure based on the combined outputs of both spectral method and the corresponding results obtained from the average empirical relation method. Afterwards, an average was calculated for each point. Also, the map (Figure 10) supports geological interpretation and exploration efforts, and aids in identifying regions of thicker or thinner crust, which can be crucial for understanding geological processes, resource potential, and geo-hazard assessment in the study area

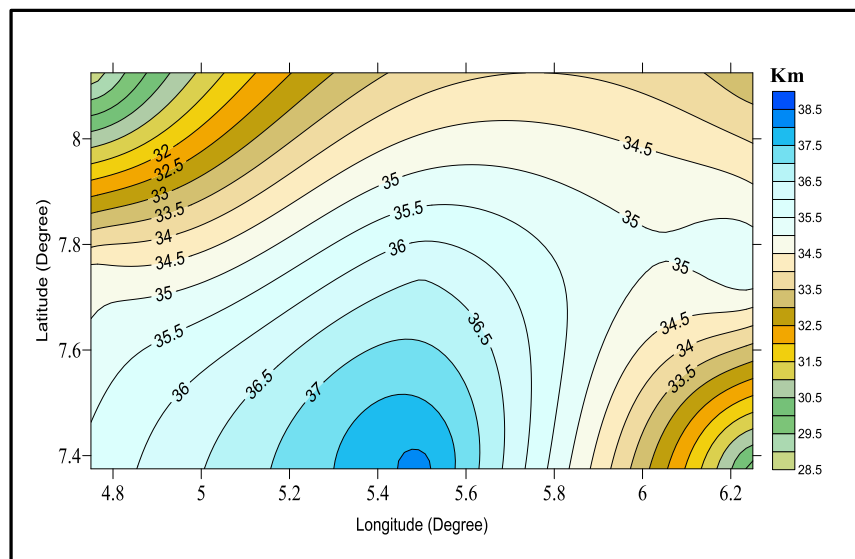


Figure 9: Contour Map that Illustrates the Depth of the Moho from Power Spectral over the Study Area. [Contour Interval is 0.5 km. Colour Bar at the Right Indicate Values of the Crustal Thickness in the Area]

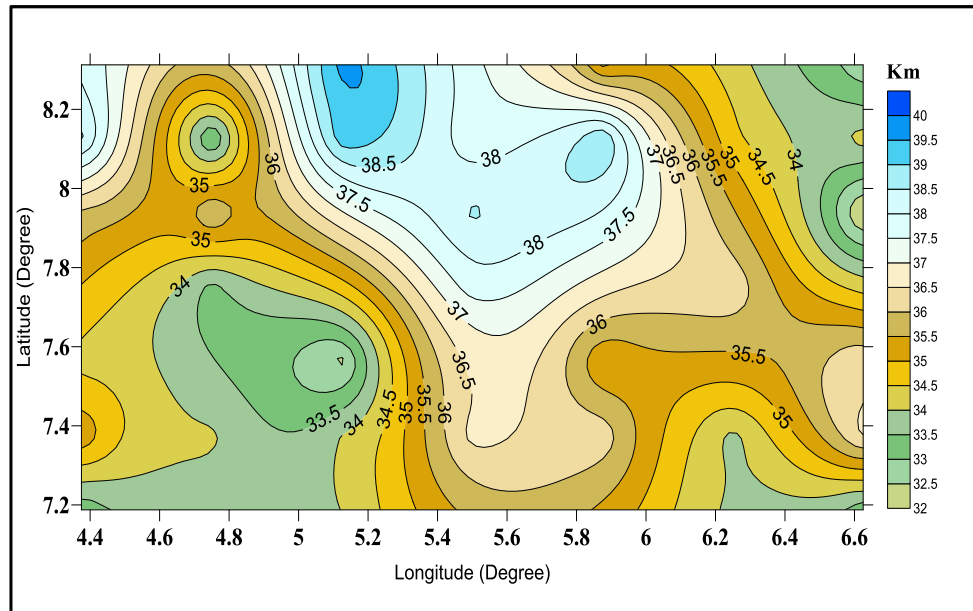


Figure 10: Final Crustal Thickness Contour Map of the Study Area. Contour Interval Is 0.5 Km. Colour Bar at the Right Indicate Values of the Crustal Thickness in the Area

The crustal thickness across the study area was observed to range from 32 km to 40 km, aligning with previous findings for Nigeria (Daniyan et al., 2002). To facilitate easy estimation of crustal thickness at any point within the study area based on Bouguer anomaly values, a formula was sought. Average crustal thickness values obtained from spectral and empirical methods were paired with corresponding Bouguer anomaly values for different points in the study area. These pairs were plotted on a graph (Figure 11), where crustal thickness (H_C) in kilometers was plotted against Bouguer anomaly (BG) values in mGal. The plotted data exhibited a linear relationship between crustal thickness and Bouguer anomaly values. A straight line equation was derived from this relationship through regression analysis. The resulting equation derived from the plot is:

$$H_C = 34.39 - 0.175BG \quad (22)$$

Where, H_C is crustal thickness in kilometres
 BG= Bouguer anomaly values in mGal.

This formula allows for the estimation of crustal thickness at any point within the study area based on the Bouguer anomaly value measured at that point. It provides a practical tool for geological studies, resource assessments, and understanding regional geological structures and processes. By establishing this formula, researchers and geologists can efficiently estimate crustal thickness using readily available Bouguer anomaly data, enhancing the accuracy and applicability of geological interpretations and investigations within the study area.

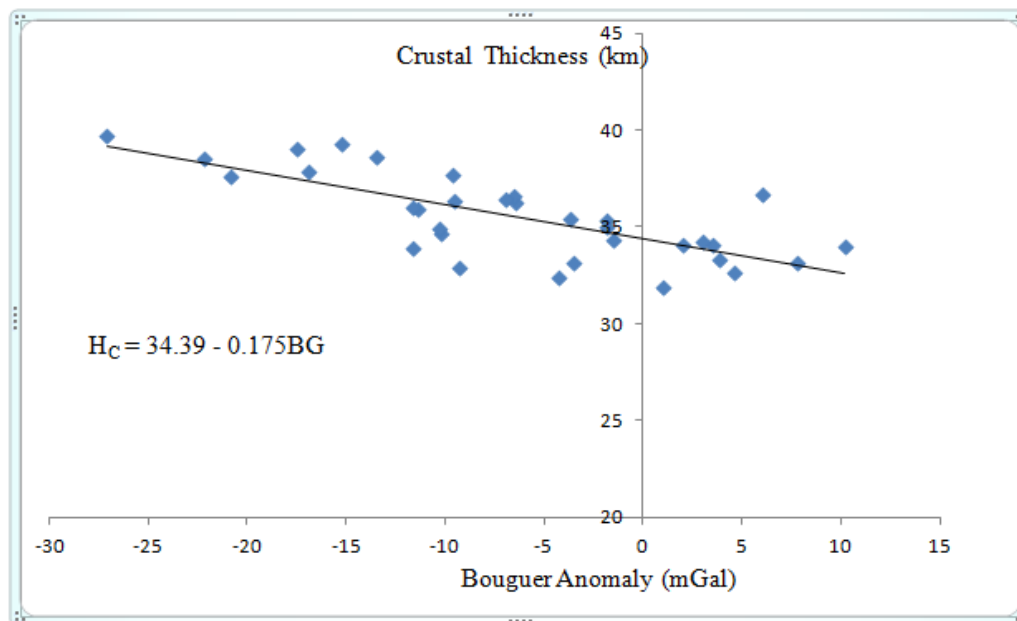


Figure 11: Graph of Crustal Thicknesses against Bouguer Anomaly Values

Stability of the Study Area

Plate tectonics is a scientific theory that explains the large-scale movements of Earth's lithosphere, as established by Brown and Girdler in 1980. It builds upon the earlier concept of continental drift proposed by Alfred Wegener. The lithosphere, which constitutes the rigid outer shell of Earth, is fragmented into tectonic plates. While definitions may vary, there are generally considered to be seven or eight major plates, along with numerous minor plates. The relative motion of these plates and their interactions at plate boundaries—whether convergent (colliding), divergent (moving apart), or transform (sliding past each other)—determine geological features such as earthquakes, volcanic activity, mountain formation, and the creation of oceanic trenches (Hofstetter et al., 2000). The dynamic movement of tectonic plates can result in collisions, separations, or lateral movements. Plate boundaries, where these interactions occur, are focal points for geological activity. For example, earthquakes and volcanic eruptions often stem from the energy released during these interactions (Hofstetter et al., 2000). Africa, notably, is positioned on a stable continental plate, which contributes to its relative lack of seismic

activity compared to regions situated on more active plate boundaries. The study area under consideration forms part of a significant inland sedimentary basin within Nigeria. Nigeria itself resides on the stable African plate. The crustal thickness observed in the study area, ranging from 32 km to 40 km, aligns closely with the crustal thickness of the broader African continent as depicted in global Moho maps (Figure 12). This thickness is indicative of a stable tectonic setting, which contributes to the overall stability of the region. In regions characterized by thicker crust, such as observed in the study area, the enhanced stability can be attributed to the structural strength provided by the thicker lithospheric layer. This stability reduces the likelihood of tectonic activity such as earthquakes and volcanic eruptions, thereby influencing the overall geological and environmental conditions of the area. Understanding crustal thickness and its relationship to tectonic plate dynamics is crucial for assessing regional stability, geological hazards, and resource potential. The study of these factors contributes to a comprehensive understanding of Earth's geological processes and their impacts on human societies and natural environments.

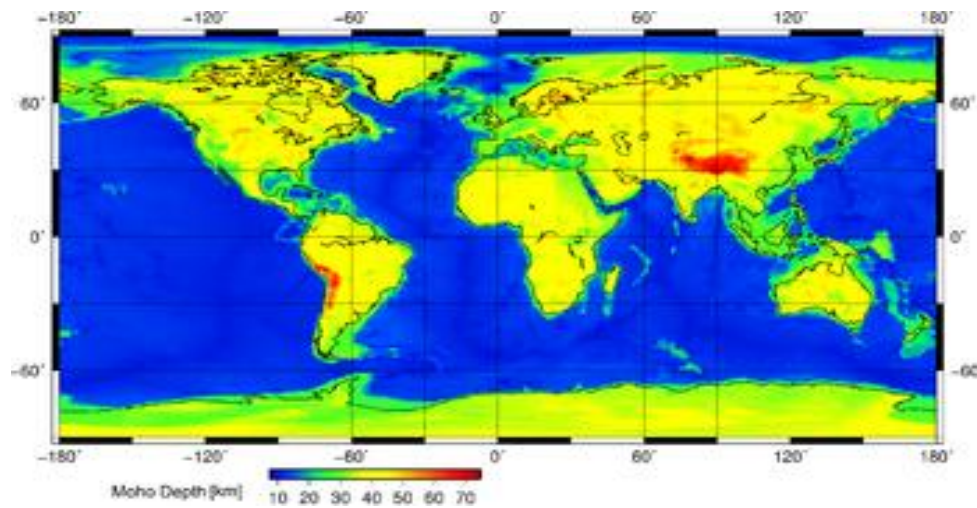


Figure 12: Moho Map of the World (Internet Source)

CONCLUSION

In conclusion, the Bouguer gravity anomaly map of the study area provides crucial insights into its geological characteristics and tectonic activities. The map reveals continuous anomalies with spherical shaped closures and uninterrupted lineaments trending NE-SW, indicating major discontinuities associated with geological structures and uplifted areas. These anomalies are pivotal for delineating boundaries and understanding the geological history of the region. Negative anomalies on the Bouguer anomaly map are attributed to low-density bodies or thick sedimentary covers, whereas positive anomalies towards SW, SE, and NE suggest high-density bodies or intrusive features beneath shallow sediments. This information aids in deciphering the subsurface geological framework and is invaluable for predicting future geological movements and conducting tectonic studies. The empirical relation method, though useful, shows more irregularities in crustal thickness estimates compared to the power spectral method. This discrepancy is likely due to the empirical method's reliance on mathematical models rather than direct geophysical data from the field. In contrast, the spectral method offers more reliable results with steadier fluctuations in crustal thickness, providing a clearer depiction of subsurface variations. Figure 10, presenting the exact crustal thickness across the study area ranging from 32 km to 40 km, closely aligns with the overall crustal thickness observed across Nigeria. This consistency reinforces the stability of the region, supported by adequate crustal thickness which mitigates geological hazards. In summary, the integrated approach using Bouguer gravity anomaly mapping, empirical relations, and spectral analysis enhances our understanding of the study area's geological dynamics. It underscores the importance of advanced geophysical methods in geological studies, offering critical insights for resource exploration, hazard assessment, and

environmental management. Further research and application of these methods will continue to refine our knowledge of Earth's processes and their impact on regional geological settings.

REFERENCES

- Ajakaiye, D. E., & Ojo, S. B. (1989). Preliminary Interpretation of Gravity Measurement in the Nupe Basin Area. Lagos, Nigeria. *Elizabethan Publish*.
- ASTM, L. (2010). Standard Guide for Using the Gravity Method for Subsurface Investigation, ASTM International, West Conshohocken
- Bansal, A. R., & Dimri, V. P. (2001). Depth Estimation from the Scaling Power Spectral Density of Non Stationary Gravity Profile. *Pure and Applied Geophysics*, 158, 799–812.
- Braide, S. P. (1992). Geological Development Origin and Energy of Mineral Resources Potential of the Lokoja Formation in the Southern Bida Basin. *Journal of Mining and Geology*, 28, 33-44.
- Bauer, P. W., Johnson, P. S., & Kelson, K. I. (1999) Geology and hydrogeology of the southern Taos valley, Taos County, New Mexico: Socorro, New Mexico Bureau of Geology and Mineral Resources, Final Technical Report to New Mexico Office of the State Engineer, 56 pages, 4 plates.
- Brown, C., & Girdler, R. W. (1980). Interpretation of African Gravity and its Implication for the Breakup of the Continent. *Journal of Geophysics*, 85, 6443-6444.
- Daniyan, M. A., Udensi, E. E., Ajakaiye, D. E., & Ige, T. E. (2002). The Crustal Thickness in Nigeria: Preliminary Result from Bouguer Gravity

- Anomaly Data. *Nigerian Journal of Technological Research*, 1, 25-31
- Demenitskaya, R. M. (1958). Planetary Structure and their Reflection in Bouguer Anomaly. *Geology Bulletin*, 8.
- Hofstetter, A., Dorbath, C., Rybakov, M. & Goldmid, V. (2000). Crustal and Upper Mantle Structure across the Dead Sea Rift and Israel from Teleseismic P-Wave Tomography and Gravity Data. *Tectonophysics*, 327, 37-59.
- Lewis, B. R. T. (1983). The Process of Formation of Ocean Crust. *Science*, 220, 151-157, doi: 10.1126/science.220.4593.151.
- Mishra, D. C. (2000). Gravity Anomaly. National Geophysical Research Institute, Hyderabad, India. *Geophysics and Geochemistry*, 3.
- Obaje, N. G., Musa, M. K., Odoma, A. N., & Hamza, H. (2009). The Bida Basin in North Central Nigeria. Sedimentology and Petroleum Geology. *Journal of Petroleum and Gas Exploration Research*, 1(1), 1-13.
- Obaje, N. G., Moumouni, A., Goki, N. G., & Chanda, M. S. (2011). Stratigraphy, Paleogeography and Hydrocarbon Resource Potentials of the Bida Basin in North Central Nigeria. *Journal of Mining and Geology*, 47(2), 97-114.
- Olusola, J. O., Suraj, A. A., Temitope, M. A., & Aminat, O. A. (2011). Sedimentological and Geochemical Studies of Maastrichtian Clays in Bida Basin, Nigeria: Implication for Resource Potential. *Centre point Journal*, 17(2), 71-88.
- Poudjom Djomani, Y.H., Diament M. & Albouy Y., (1992). Mechanical Behaviour of the Lithosphere Beneath the Adamawa Uplift, Cameroon, West Africa, Based on Gravity Data. *Journal of African Earth Sciences*, 15, 81-90.
- Shekwolo, P. D. (1992). Regional Hydrogeology of Bida Basin. *Unpublished (Ph.D.Thesis)*. Ahmadu Bello University, Zaria, Nigeria.
- Spector, A., & Grant, F.S. (1970). Statistical Models for Interpreting Aeromagnetic Data. *Geophysics*, 35, 293-302.
- Syberg, F. J. R. (1972). A Fourier Method for the Regional-Residual Problem of Potential Fields. *Geophysics Prospective*, 20, 47-75.
- Tealeb, A., & Riad, S. (1986). Regional Tectonics of Sinai Peninsula Interpreted from Gravity and Deep Seismic Data. *E. G .S. 5th Annual Meeting*, 29(30), 18-49.
- Woolland, G. P. (1959). Crustal Structure from Gravity and Seismic Measurements. *Geophysics Research*, 64 (10), 152-154.
- Woolland, G. P. & Strange, W. E. (1962). Gravity Anomalies and Crust of Earths in the Pacific Basin. *Geophysical Monograph*, 6, 60-80.